Current-driven domain wall motion in cylindrical nanowires

R. Wieser,[1] E. Y. Vedmedenko,[1] P. Weinberger,[2] and R. Wiesendanger[1]
[1]*Institut für Angewandte Physik und Zentrum für Mikrostrukturforschung, Universität Hamburg, Jungiusstrasse 11, D-20355 Hamburg, Germany*
[2]*Center for Computational Nanoscience, Seilerstätte 10/22, A-1010 Vienna, Austria*
(Received 25 February 2010; revised manuscript received 7 September 2010; published 20 October 2010)

Current driven motions of domain walls in ferromagnetic, cylindrical nanowires are investigated by solving the Landau-Lifshitz-Gilbert equation including the adiabatic and nonadiabatic spin torque terms. Depending on the type of domain wall (transverse or vortex) and on the nonadiabaticity parameter β different behavior of the domain wall motion has been found. A transverse domain wall shows a linear motion accompanied by a clock- or anticlockwise precession of the wall depending on the relation between the nonadiabaticity parameter β and the Gilbert damping α. For $\alpha=\beta$ no rotation occurs. Further, an easy way to derive the velocity equation is presented. In the case of the vortex domain wall an unexpected chirality effect has been found. Depending on the sense of rotation either a straight motion or a reversal of the rotation followed by a straight motion can be seen. Furthermore, due to the impossibility of a Walker breakdown the averaged velocity of the domain wall v is zero for all currents with $\beta=0$ while the motion is damped by the emission of spin waves for higher currents and $\beta>\alpha$.

DOI: 10.1103/PhysRevB.82.144430 PACS number(s): 75.78.−n, 75.40.Mg, 75.60.Ch

I. INTRODUCTION

New concepts in the field of data storage media[1–4] and logic devices[5] put magnetic nanowires into the focus of interest. In the case of nanowires and other future magnetoelectronic devices domain wall motions are important because their switching and manipulation can easily be controlled. During the last few years in particular domain walls in artificial permalloy nanostructures have been investigated intensively.[2,6,7] It has been shown that depending on the aspect ratio two types of domain walls occur, namely, transverse domain walls (TDW), which are similar to a Néel wall, and more complex vortex domain walls (VDW). Both types of domain walls can be found also in cylindrical nanowires.[8–11] The difference between both concepts of wire architecture leads to differences in the magnetization dynamics. It has been postulated recently that field driven vortex domain walls in flat nanowires show complex motions.[6,7] Later similar results were obtained for current-driven domain walls.[12] In contrast to flat structures vortex domain walls in cylindrical nanowires move uniformly,[9,11] which in turn should be more convenient for applications. Yan *et al.*[13] made a detailed numerical investigation of the motion of the TDW in cylindrical nanowires. It could be shown that the TDW shows a similar dynamics as in the field driven case. Further, it has been shown that the TDW has a velocity which is proportional to the applied current. The same result has been proposed by Mougin *et al.*[14] for the velocity of a TDW just after the Walker breakdown. While the dynamics of domain walls in one-dimensional (1D) structures and flat nanowires is rather well understood,[14–18] there is much less information on the domain wall velocity in cylindrical wires. In this publication we show an easy way to derive the velocity equations of a TDW in a uniaxial cylindrical nanowire. Further we point out that in the case of a biaxial anisotropy the velocity of the TDW changes and become similar to the velocity of the VDW. Another important point, which has been found in terms of numerical simulations, is that field driven vortex domain walls in cylindrical nanowires do not show a so-called Walker breakdown[8] as is the case in biaxial transverse domain wall systems.[14,15,19] Instead a reduction in the velocity due to the emission of spin waves (SW) has been found.[8] In this manuscript, we generalize this effect to the case of current driven vortex domain walls in a cylindrical wire geometry.

The paper is organized as follows. In Sec. II we give a description of the underlying model. Section III gives an overview of the results of transverse domain walls in cylindrical wires. These results are already published in.[13] Here we present an alternative way just by simple deductions to get exactly the same results. Section IV is devoted to the investigation of the motion of vortex domain walls, followed by a summary (Sec. V).

II. MODEL

Since we do not intend to describe a particular material the following Heisenberg Hamiltonian:

$$\mathcal{H} = -J\sum_{\langle ij\rangle} \mathbf{S}_i \cdot \mathbf{S}_j - D_z\sum_i (S_i^z)^2 - \omega\sum_{i<j} \frac{3(\mathbf{S}_i \cdot \mathbf{e}_{ij})(\mathbf{e}_{ij} \cdot \mathbf{S}_j)}{r_{ij}^3} \tag{1}$$

is applied, where $S_i=\mu_i/\mu_s$, $\mu_s=|\mu_i|$, is the direction of the magnetic moment μ_i at site i, S_i^z being its z component along the wire. The first sum in Eq. (1) corresponds to an exchange interaction between first nearest neighbors with a ferromagnetic coupling constant $J>0$, the second one to a uniaxial anisotropy term with the z axis as the easy axis of the system, and the last one to a magnetic dipole-dipole interaction. In Eq. (1)

$$\mathbf{e}_{ij} = (\mathbf{R}_i - \mathbf{R}_i)/r_{ij}, \quad r_{ij} = |\mathbf{R}_i - \mathbf{R}_i|; \quad \omega = \mu_0 \mu_s^2/(4\pi a^3), \tag{2}$$

where the $\mathbf{R}_i$ refers to the lattice positions in a simple cubic lattice of spacing a. In the following $D_z=0.005J$, $\omega=0.2J$, and all energies will be given in units of J.

For the equation of motion of the magnetic moments caused by a current in z direction a modified Gilbert equation that includes spin torque terms was suggested[20–22]

$$\frac{\partial \mathbf{S}_i}{\partial t} = -\frac{\gamma}{\mu_s}\mathbf{S}_i \times \mathbf{H}_i + \alpha \mathbf{S}_i \times \frac{\partial \mathbf{S}_i}{\partial t} - [(\mathbf{u}\cdot\nabla)\mathbf{S}_i] + \beta \mathbf{S}_i \times [(\mathbf{u}\cdot\nabla)\mathbf{S}_i], \tag{3}$$

where $\gamma=g\mu_B/\hbar$ is the gyromagnetic ratio, $\mathbf{H}_i=-\partial\mathcal{H}/\partial\mathbf{S}_i$ the internal field, α the Gilbert damping factor, and $u=|\mathbf{u}|$ is given by

$$u = j_e P g \mu_B/(2eM_s); \quad M_s = \mu_s/a^3 \tag{4}$$

with j_e being the current density, P the polarization, M_s the saturation magnetization, and β the nonadiabaticity parameter. Written in the form of Eq. (3), one can immediately see that for $u=0$ the "usual" Gilbert form is recovered. Due to the time derivative on both sides this differential equation is not easy to manage. To get a more manageable equation one has to transform this Gilbert equation into a modified Landau-Lifshitz-Gilbert equation. Therefore, the product $\mathbf{S}_i\times$ is usually added to both sides of Eq. (3) which leads to

$$\mathbf{S}_i \times \frac{\partial \mathbf{S}_i}{\partial t} = -\frac{\gamma}{\mu_s}\mathbf{S}_i \times (\mathbf{S}_i \times \mathbf{H}_i) + \alpha \mathbf{S}_i \times \left(\mathbf{S}_i \times \frac{\partial \mathbf{S}_i}{\partial t}\right) - [(\mathbf{u}\cdot\nabla)\mathbf{S}_i] + \beta \mathbf{S}_i \times [(\mathbf{u}\cdot\nabla)\mathbf{S}_i]. \tag{5}$$

Inserting the last expression into Eq. (3) and using the rule $\mathbf{a}\times(\mathbf{b}\times\mathbf{c})=\mathbf{b}(\mathbf{a}\cdot\mathbf{c})-\mathbf{c}(\mathbf{a}\cdot\mathbf{b})$

$$\mathbf{S}_i \times \left(\mathbf{S}_i \times \frac{\partial \mathbf{S}_i}{\partial t}\right) = \underbrace{\left(\mathbf{S}_i \cdot \frac{\partial \mathbf{S}_i}{\partial t}\right)}_{=0} - \mathbf{S}_i^2 \frac{\partial \mathbf{S}_i}{\partial t} = -\frac{\partial \mathbf{S}_i}{\partial t} \tag{6}$$

(the first term on the right-hand side vanishes because of the orthogonality $\frac{\partial \mathbf{S}_i}{\partial t} \perp \mathbf{S}_i$) one gets

$$(1+\alpha^2)\frac{\partial \mathbf{S}_i}{\partial t} = -\frac{\gamma}{\mu_s}\mathbf{S}_i \times [\mathbf{H}_i + \alpha(\mathbf{S}_i \times \mathbf{H}_i)] - (\mathbf{u}\cdot\nabla)\mathbf{S}_i - (\alpha-\beta)\mathbf{S}_i \times [(\mathbf{u}\cdot\nabla)\mathbf{S}_i] + \alpha\beta \mathbf{S}_i \times (\mathbf{S}_i \times [(\mathbf{u}\cdot\nabla)\mathbf{S}_i]). \tag{7}$$

This equation can be simplified to

$$\mathbf{S}_i \times (\mathbf{S}_i \times [(\mathbf{u}\cdot\nabla)\mathbf{S}_i]) = \underbrace{(\mathbf{S}_i \cdot [(\mathbf{u}\cdot\nabla)\mathbf{S}_i])}_{=0}\mathbf{S}_i - \mathbf{S}_i^2[(\mathbf{u}\cdot\nabla)\mathbf{S}_i] = -[(\mathbf{u}\cdot\nabla)\mathbf{S}_i]. \tag{8}$$

Here we have used the fact that $(\mathbf{u}\cdot\nabla)\mathbf{S}_i \perp \mathbf{S}_i$. Finally, one gets the modified Landau-Lifshitz-Gilbert (LLG) equation[15]

$$\frac{\partial \mathbf{S}_i}{\partial t} = -\frac{\gamma}{(1+\alpha^2)\mu_s}\mathbf{S}_i \times \mathbf{H}_i - \frac{\alpha\gamma}{(1+\alpha^2)\mu_s}\mathbf{S}_i \times (\mathbf{S}_i \times \mathbf{H}_i) - \frac{\alpha-\beta}{(1+\alpha^2)}\mathbf{S}_i \times [(\mathbf{u}\cdot\nabla)\mathbf{S}_i] + \frac{1+\alpha\beta}{(1+\alpha^2)}\mathbf{S}_i \times (\mathbf{S}_i \times [(\mathbf{u}\cdot\nabla)\mathbf{S}_i]) \tag{9}$$

which is identical to the usual LLG equation in the limit of $u\to 0$.

III. TRANSVERSE DOMAIN WALLS

A quick inspection of Eq. (9) already leads to interesting conclusions. According to Eq. (1) a relaxation of transverse domain walls in cylindrical wires leads to a "translational" and "rotational invariance" of the dynamics of such domain walls since $\mathbf{S}_i\times\mathbf{H}_i=0$, i.e., since the first and second term in Eq. (9), describing the precession and the relaxation due to the internal field $\mathbf{H}_i$, do not contribute to the time evolution of the magnetic moments. In this particular case the time evolution appears entirely due to the terms induced by the electric current, namely, the third (relaxation) and fourth (precession) term in Eq. (9). If an additional hard axis anisotropy is present the situation changes: a rotation of the domain wall leads to a change in the internal field $\mathbf{H}_i$. Furthermore, depending on the sign of $\alpha-\beta$, the fourth term describes either a clockwise ($\alpha-\beta>0$) or an anticlockwise ($\alpha-\beta<0$) rotation. For $\beta=\alpha$ the precessional term is zero, and the time evolution is described solely by a direct reversal of the magnetization. In this particular case the velocity of the domain wall can be read off directly from the prefactor of the remaining third term, i.e.,

$$v_{\beta=\alpha} = u. \tag{10}$$

In the case $\alpha\neq\beta$, a similar deduction leads to the two decoupled terms on the right-hand side of Eq. (9). The first term (initially the third term) is responsible for the precession. The second term (initially the fourth term) is responsible for the relaxation. Due to the mentioned decoupling above the velocity can be obtained directly from the prefactor of the relaxation term

$$v_{\mathrm{TDW}} = \frac{1+\beta\alpha}{(1+\alpha^2)}u. \tag{11}$$

The precessional term in Eq. (9) leads to a decoupled rotation of the out-of-plane components of TDW's with a precession speed equal to

$$v_{\mathrm{prec.}} = \frac{\alpha-\beta}{1+\alpha^2}u \tag{12}$$

the sense of rotation as already mentioned being determined by the sign of $\alpha-\beta$. It is important to notice that these velocity Eqs. (11) and (12) describe the motion of a current driven TDW performing a precessional motion. The results are independent on the wire geometry, similar results could be found also for thin-film geometries, quadratic rods or lin-

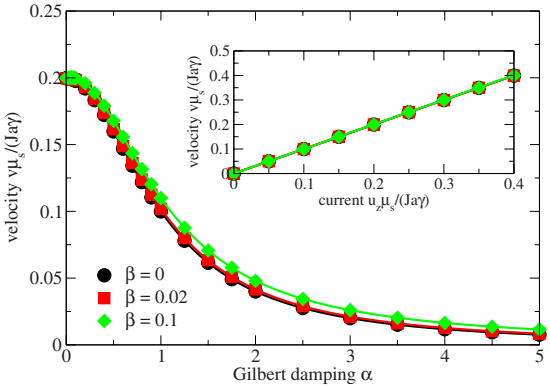

FIG. 1. (Color online) Domain wall velocity of a TDW as a function of the Gilbert damping α for different values of β in cylindrical wires. Here $u=0.2$ is assumed. The inset shows the velocity as a function of u for $\alpha=0.02$.

ear chains.[16–18] The only condition which has to be fulfilled is just precession of the domain wall. That means that a current driven TDW after the Walker breakdown moves with a velocity which can be calculated using Eq. (11) (see Refs. 14 and 23).

To test the above analytical reasoning we have performed numerical spin dynamics simulations. In the following we present results of the simulations for cylindrical nanowires oriented parallel to the z axis. The wires are considered to consist out of a set of lattice sites forming a cylinder of length $1024d_1$ and diameter $8d_2$, where d_1 and d_2 are the interlayer and next nearest-neighbor distance, respectively. For TDW's the results of the simulations performed for wires or linear chains of the same length led to identical results caused by the quasi-1D behavior of such objects. Due to the shape and the crystalline magnetic anisotropy the equilibrium magnetization is aligned along the long axis of the system (z axis). The current flow is along the wire (z axis) which means that $\mathbf{u}\cdot\nabla=u_x\frac{\partial}{\partial x}+u_y\frac{\partial}{\partial y}+u_z\frac{\partial}{\partial z}$ becomes $\mathbf{u}\cdot\nabla=u_z\frac{\partial}{\partial z}$ and, hence, $u=u_z$. The simulations have been started with a relaxed TDW ($\omega/J=0$) or VDW ($\omega/J=0.2$).[8,9] Switching on the current leads to the acceleration of the domain wall. The velocity of this motion can be calculated from the time dependence of the magnetization as

$$v=\frac{N}{2}\frac{\mathrm{d}\bar{S}_N^z}{\mathrm{d}t},\quad \bar{S}_N^z=\sum_{n=1}^{N}S_n^z, \tag{13}$$

where N refers to the number of atomic planes intersecting the chosen cylinder.

Figure 1 shows the velocity v_{TDW} of a TDW, as a function of the Gilbert damping α for different nonadiabaticity parameters β. The filled symbols correspond to the numerical data while the solid lines are the analytical results given in Eq. (11). In the inset the corresponding velocity curves are displayed as a function of the current u.

From Fig. 1 it can be seen that the influence of β on the velocity is rather small whereas a change in the Gilbert damping causes a sizeable change in the velocity. It should be noted that in Fig. 1 v_{TDW} is directly proportional to u [see the prefactor of the third term in Eq. (9)] and is identical to the velocity of a TDW after the Walker breakdown.[14] This remarkable fact means that during the motion of a TDW any relaxations via precessions of the magnetization are absent. Thus, in contrast to the usual picture of domain wall motions in which both, precessional and relaxation movements occur simultaneously, they are decoupled in TDW's formed in cylindrical wires.

Figure 2 shows the time evolution of the out-of-plane components of the magnetization profile of a TDW corresponding to $\alpha=0.02$,

$$M_x=\sin\phi\ \mathrm{sech}\frac{z}{\delta},\quad M_x=\cos\phi\ \mathrm{sech}\frac{z}{\delta}, \tag{14}$$

where ϕ is the time-dependent azimuthal angle and δ the domain wall width. The sense and the velocity of the precession can be obtained by analyzing the time evolution of the height of the sech peaks. In Fig. 2(a) one sees a slow clockwise rotation ($\alpha-\beta=0.02>0$) while in Fig. 2(b) a faster anticlockwise rotation ($\alpha-\beta=0.02-0.1<0$). In the case corresponding to $\alpha=\beta$ our simulations show a straight domain wall motion without any precession. These results are in excellent agreement with the analytical prediction Eq. (12). In realistic materials $\alpha\neq\beta$. For instance the values of $\alpha=0.01$ and $\beta\approx0.13$ reported for permalloy[24] imply an anticlockwise rotation in wire made out of this material. It seems that the sense and the speed of the rotation can be manipulated by doping of this alloy, e.g., with holmium.[24] Unfortunately, this also leads to a decrease in the domain wall velocity.

In a recent publication[13] the authors call this type of domain wall massless in the presence of an external field. The reason is that the missing hard axis anisotropy, as in thin film structures, leads to the precession of the domain wall. Therefore, there is no change in the domain wall energy and corresponding effective mass $m^*:E(v\neq0)-E(v=0)=\frac{1}{2}m^*v^2$ is equal to zero. Here E is the domain wall energy and v the velocity of the domain wall. This means that there is no

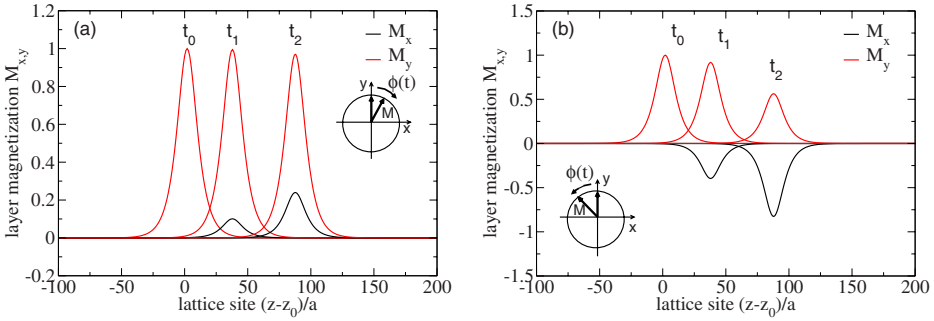

FIG. 2. (Color online) Time evolution of the out-of-plane components of a TDW corresponding to $u=0.2$, $\alpha=0.02$ and (a) $\beta=0$, (b) $\beta=0.1$; $t_0<t_1<t_2$ are equidistant steps in time. The wire cross sections are depicted in the insets.

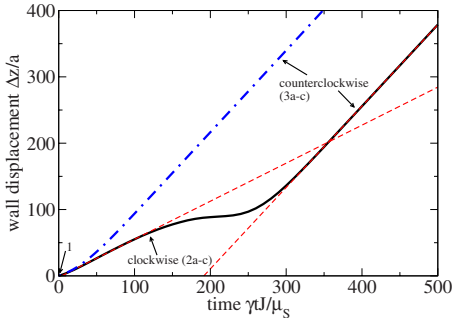

FIG. 3. (Color online) Current driven domain wall motion of a VDW: wall displacement as function of time for a VDW with counterclockwise sense of rotation (dotted-dashed line) and a VDW with clockwise sense of rotation in the beginning (solid line). The current flow is along the wire in $+z$ direction (u=0.35, α=0.02, β=0.1, and ω/J=0.07). The dashed lines are guide for the eyes. The slopes of these lines are equal to the velocity of the VDW. The numbers 1, $2a-c$ and $3a-c$ correspond with the pictures in Fig. 4.

change in the shape of the domain wall during motion. In this case the driving field leads to the precession of the domain wall (see, Refs. 9 and 25) We, however, did not use any external field leading to a energy change. Current driven domain wall motion appears just due to the conservation of momentum and, therefore, there is no change neither in the domain wall energy nor in the mass.

The dynamics of domain wall changes in the case of biaxial TDW's.[15,26] Here, a direct reversal occurs. This means that the velocity equation applying to TDW's with uniaxial anisotropy is no longer valid because now the first two terms in Eq. (9) do not remain constant in time. In this case the velocity equation coincides with that of domain walls in a planar film geometries[22]

$$v = \frac{\beta}{\alpha} u. \tag{15}$$

IV. VORTEX DOMAIN WALLS

In the case β=0 a vortex domain wall passes a small distance and then stops: there is no further domain wall motion, i.e., $v(u)$=0, for the current values used in our simulations. The reason is the compensation of the microscopic torques in a perfect vortex. This phenomenon is in agreement with previous simulations of biaxial transverse domain walls.[15,22] A domain wall motion above a certain critical current has not been investigated. Nontrivial results occur for $\beta \neq 0$. Here one has to distinguish between two cases, which correspond to the two senses of rotation and the direction of motion. Figure 3 shows the wall displacement of a VDW with a counterclockwise (dotted-dashed line) and with clockwise sense of rotation (solid line). The dash lines are just guide for the eyes. Figure 4 shows the cross section of the wire at different times: 1: clockwise rotation of the VDW at time $\gamma tJ/\mu_S$=0 (Δz=0), 2a–2c: VDW with clockwise rotation passing the 480th layer (Δz=30a) at $\gamma tJ/\mu_S \approx 90$, and 3a–3c: after rotation reversal (Δz=250a, $\gamma tJ/\mu_S \approx 400$). The

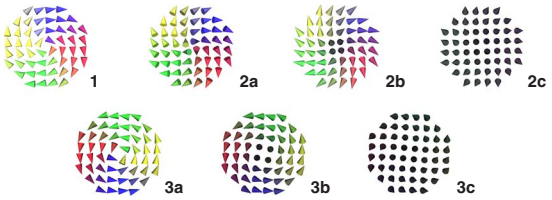

FIG. 4. (Color online) Current driven domain wall motion of a VDW: crossection of the wire, at different times and different layers. 1: clockwise VDW at time $\gamma tJ/\mu_S$=0, 2a–2c: moving clockwise VDW passing the 480th layer at $\gamma tJ/\mu_S \approx 90$ (a to c: equidistant time steps) and 3a–3c: counterclockwise VDW after changing the sense of rotation (passing the 700th layer at $\gamma tJ/\mu_S \approx 400$, a to c: equidistant time steps).

domain wall moves in $+z$ direction, which corresponds to a movement in the direction of the observer. In the case of the VDW with clockwise rotation one sees a linear displacement followed by a small backward motion and an additional linear motion at the end. During the backward motion the sense of rotation changes from clockwise to counterclockwise. The same behavior occurs if one starts with one one type of VDW (clockwise or counterclockwise) and drives the domain wall in $+z$ or $-z$ direction.

The physical reason for that is the specified sense of rotation of the vector products (right-hand rule) of the precessional terms in the Landau-Lifshitz-Gilbert equation. Depending on the sense of rotation the precession terms lead to a clockwise or counterclockwise rotation of the magnetic moment. Due to the double cross products the relaxation terms do not distinguish between different senses of rotation. These terms always lead to a linear domain wall motion in the direction of the driving force (external field or current). The direct reversal together with the clockwise or counterclockwise rotation due to the precession terms lead to different reversal paths. The first path shown in Fig. 4, 2a–2c leads to volume and surface charges. This is not the case for the second reversal's path (see Fig. 4, 3a–3c). This behavior is independent on the driving force and depends only on the rotation sense of the VDW and the direction of the vector product. Or study suggests the following rule: if the sense of rotation of the VDW (domain wall moving to the observer) is identical with the sense of rotation given by the torque between the magnetic moments and the driving force a straight domain wall motion occurs. If they are different the VDW change its sense of rotation. After that the domain wall motion becomes straight and posses the same velocity. The velocity is identical with the velocity of the biaxial TDW's

$$v_{\mathrm{VDW}} = \frac{\beta}{\alpha} u. \tag{16}$$

This agreement is because of the identical magnetization reversal mechanism (direct reversal). For $\beta=\alpha$, we find a steady-state domain wall motion with a linear increase in the domain wall velocity, $v_{\mathrm{VDW}}=u$.

The mostly fascinating result can be seen for $\beta \gg \alpha$. In this case a biaxial transverse domain wall shows typically a linear increase in the velocity followed by a Walker break-

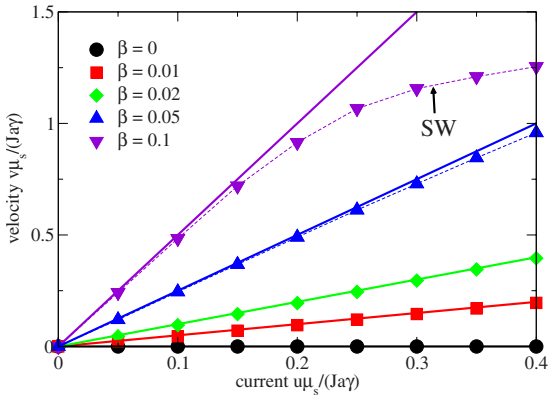

FIG. 5. (Color online) Domain wall velocity of a VDW as a function of u for different values of β. The label "SW" marks the region in which spin waves behind the domain wall occur.

down. In the case of a VDW the increase is followed by a saturation of the velocity, without any Walker breakdown. The saturation of the velocity corresponds to the emission of spin waves. In order to understand the underlying physics we calculated the so-called winding number Z,

$$Z = \frac{1}{2\pi r}\int (\text{curl}\ \mathbf{S})_z dxdy \tag{17}$$

for a wire of radius r, at each plane intersecting the wire (z =const.) and at each time step. Figure 6 shows the time dependent winding number of the 550th layer after passage of the vortex domain wall. The inset shows the winding number during the whole simulation. The peak found at $t \approx 138\gamma J/\mu_s$ marks the passage of the VDW while the subsequent oscillations of the circulation show the occurrence of SW behind the domain wall.

Identical phenomena can be observed for field driven vortex domain walls in cylindrical wires in the limit of $\alpha \to 0$ and/or large external fields.[8] Just as in the case of current-driven domain walls the spin wave is emitted due to the

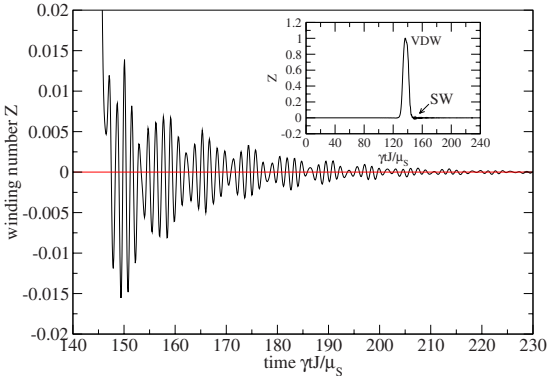

FIG. 6. (Color online) Spin wave behind a current driven VDW: winding number as function of time (at the cross section of 550th layer of the wire). Inset: the peak highlights the moment when a VDW passes the chosen layer (550th layer), the small oscillations correspond to the spin waves. These oscillations are shown in the main figure. (u=0.4, α=0.02, β=0.1)

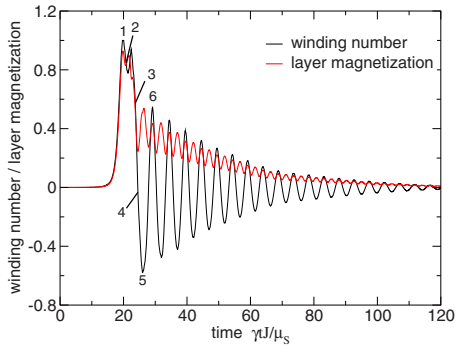

FIG. 7. (Color online) Spin wave behind a field driven VDW: winding number and perpendicular layer magnetization as function of time (fixed space: 550th layer). The numbers correspond with the pictures in Fig. 8. Here ω/J=0.2, D_z/J=0.05, $\mu_S B/J$=0.1, and α =0.02 are assumed.

impossibility of the occurrence of a Walker breakdown. In the field-driven case the energy necessary for the appearance of spin waves is due to the Zeeman term,

$$\mathcal{H}_B = -\mu_s B \sum_i S_i^z, \tag{18}$$

which describes the coupling of the magnetic moments to an external field and which has to be added to the Hamiltonian in Eq. (1).

Figure 7 shows the emitted spin wave behind the domain wall in the field driven case. Additionally to the winding number Z the perpendicular to the layer magnetization

$$M_\perp = \sqrt{M_x^2 + M_y^2} \tag{19}$$

with

$$M_\eta = \frac{1}{L}\sum_{l=1}^{L} S_l^\eta, \quad \eta = \{x,y\} \tag{20}$$

has been used to characterize the spin wave. The numbers in Fig. 7 correspond to snapshots of the cross section of the wire shown in Fig. 8. Figure 8, 1 shows the counterclockwise VDW while the Fig. 8, 2–6 correspond to snapshots of the spin wave behind the domain wall. Because of the dipolar interaction this spin wave shows a rotational symmetry, changing periodically in time. A detailed description of the spin wave emission during domain wall motion can be found in.[26]

Viewed in terms of Eqs. (1) and (9) the difference between the field driven and the current-driven domain wall motion is that in the first case the underlying principle is conservation of energy while in the second one it is the conservation of the spin torque. In the latter situation ideally no change in energy is involved. Therefore the occurrence of spin waves seems to be unexpected at the first moment. In order to shed light on this peculiar behavior one has to investigate the magnetic properties of a domain wall itself and its interaction with the current.

Figure 5 shows the domain wall profile S_z of a vortex domain wall at different radii r along the wire axis (z axis). The transversal section of the wire is depicted in the inset. A

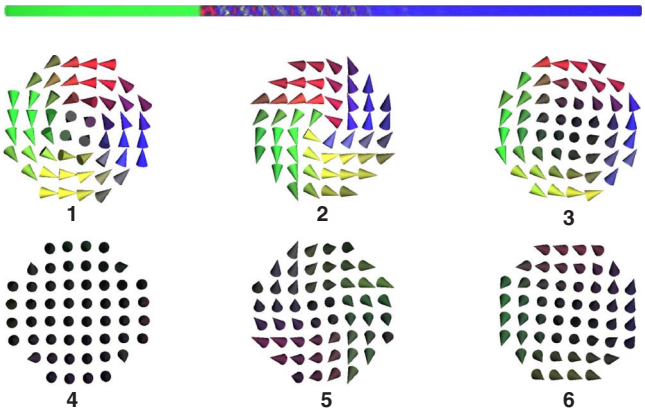

FIG. 8. (Color online) Spin wave behind a field driven VDW: Upper figure shows side view of the cylindrical wire. The domain wall with the spin wave wake behind can be clearly seen. Lower figures 1–6: cross section of the wire (550th layer) at different times. 1: VDW, 2–6: spin wave. This pictures correspond with the numbers shown in Fig. 7.

radius dependent domain wall width can be determined from the magnetization profile. The smallest domain wall width is formed along the central axis ($r=0$, central spot labeled with 1, see inset of Fig. 9). This extremely narrow part of the wall appears as a singularity (Bloch point) in the center of the VDW. With increasing radius (increasing number in Fig. 9) the domain wall width increases. Therefore, depending on the radius r, different gradients $\partial \mathbf{S}_i / \partial z$ arise in Eq. (9). This means that the current "sees" a radius-dependent spin torque (adiabatic term in the LLG equation) and also a radius-dependent reflection coefficient (nonadiabatic term). Therefore, the current leads to a deformation of the vortex, especially in the vicinity of the Bloch point. This deformation then causes a change in the domain wall energy and an emission of spin waves due to the magnetic dipole-dipole interaction, see also Fig. 6.

V. SUMMARY

In summary, current induced motions of domain walls in a cylindrical wire have been investigated. The well known fact that the nonadiabaticity parameter β plays an important role for the dynamics of a domain wall is shown to hold for cylindrical nanowires. Depending on $\alpha-\beta$ a clockwise or anticlockwise rotation of the TDW can be seen. Such a precessional motion leads to a lower velocity limit similar to the lower velocity limit of field driven domain walls.[8,25] Further, this precession protects the TDW from the Walker breakdown.

For the VDW, we show that its motion depends on the sense of rotation of the VDW in comparison to the specified sense of the cross product of the precessional term in the

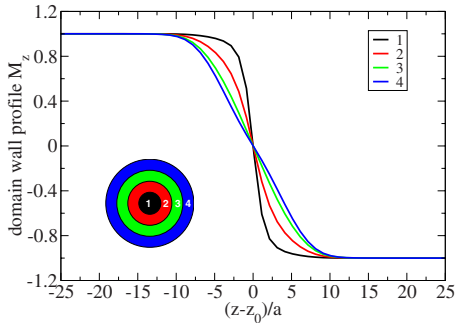

FIG. 9. (Color online) Domain wall profile (ground state: the z component of magnetization) of a vortex domain wall.

LLG Eq. (9). If the sense of rotation of the VDW is identical to that from the torque of the precessional term a straight domain wall motion with direct reversal occurs. Otherwise the VDW changes the sense of rotation and after that the same straight motion with direct reversal occurs. The relaxation terms do not affect this effect as they lead to the direct magnetization reversal which drives the domain wall in the direction of the driving force (current or external field). A Walker breakdown does not occur due to the stability of the VDW with correct sense of rotation. Therefore no continuous domain wall motions have been found provided that the spin torque is adiabatic ($\beta=0$). For $\beta>0$ the velocity of the VDW is given by the well known formula for current driven domain walls for direct reversal $v=\frac{\beta}{\alpha}u$. If $\beta=\alpha$ the negative damping due to the spin torque term and the positive damping due to the Gilbert damping α are equal and therefore a steady state motion occurs. If the nonadiabaticity is larger than the Gilbert damping, $\beta>\alpha$, we find—as expected—in the regime of small currents a linear behavior of the velocity with respect to the current and a decrease in the velocity at higher currents but no Walker breakdown. The decrease in the velocity can be explained by the emission of spin waves behind the domain wall, which in turn can be explained by considering radius-dependent domain wall widths. This leads to different gradients in Eq. (9), which in turn lead to a deformation of a vortex domain wall, especially in the center of the wire. Due to this deformation, the energy of the domain wall decreases and the energy dissipates via an emission of spin waves, implying a decrease in the kinetic energy of a vortex domain wall, and thus a decrease in velocity.

ACKNOWLEDGMENTS

The authors thank C. Schieback and N. Mikuszeit for helpful discussions. This work has been supported by the Deutsche Forschungsgemeinschaft in the framework of the project B3 of the SFB 668 and the Cluster of Excellence "Nanospintronics."

[1] S. Krause, G. Herzog, T. Stapelfeldt, L. Berbil-Bautista, M. Bode, E. Y. Vedmedenko, and R. Wiesendanger, Phys. Rev. Lett. **103**, 127202 (2009).
[2] S. S. P. Parkin, M. Hayashi, and L. Thomas, Science **320**, 190 (2008).
[3] C. A. Ross, R. W. Chantrell, M. Hwang, M. Farhoud, T. A. Savas, Y. Hao, H. I. Smith, F. M. Ross, M. Redjdal, and F. B. Humphrey, Phys. Rev. B **62**, 14252 (2000).
[4] K. Nielsch, R. B. Wehrspohn, J. Barthel, J. Kirschner, S. F. Fischer, H. Kronmüller, T. Schweinböck, D. Weiss, and U. Gösele, J. Magn. Magn. Mater. **249**, 234 (2002).
[5] D. A. Allwood, G. Xiong, C. C. Faulkner, D. Atkinson, D. Petit, and R. P. Cowburn, Science **309**, 1688 (2005).
[6] M. Kläui, J. Phys.: Condens. Matter **20**, 313001 (2008).
[7] A. Thiaville and Y. Nakatani, in *Spin Dynamics in Confined Magnetic Structures III*, edited by B. Hillebrands and A. Thiaville (Springer, Berlin, Heidelberg, 2006).
[8] R. Wieser, U. Nowak, and K. D. Usadel, Phys. Rev. B **69**, 064401 (2004).
[9] R. Wieser, U. Nowak, and K. D. Usadel, Phase Transitions **78**, 115 (2005).
[10] H. Forster, T. Schrefl, D. Suess, W. Scholz, V. Tsiantos, R. Dittrich, and J. Fidler, J. Appl. Phys. **91**, 6914 (2002).
[11] R. Hertel and J. Kirschner, Physica B **343**, 206 (2004).
[12] S.-M. Seo, K.-J. Lee, W. Kim, and T.-D. Lee, Appl. Phys. Lett. **90**, 252508 (2007).
[13] M. Yan, A. Kákay, S. Gliga, and R. Hertel, Phys. Rev. Lett. **104**, 057201 (2010).
[14] A. Mougin, M. Cormier, J. P. Adam, P. J. Metaxas, and J. Ferrè, EPL **78**, 57007 (2007).
[15] C. Schieback, M. Kläui, U. Nowak, U. Rüdiger, and P. Nielaba, Eur. Phys. J. B **59**, 429 (2007).
[16] S. Zhang and Z. Li, Phys. Rev. Lett. **93**, 127204 (2004).
[17] M. E. Lucassen, H. J. van Driel, C. M. Smith, and R. A. Duine, Phys. Rev. B **79**, 224411 (2009).
[18] S. E. Barnes and S. Maekawa, Phys. Rev. Lett. **95**, 107204 (2005).
[19] N. L. Schryer and L. R. Walker, J. Appl. Phys. **45**, 5406 (1974).
[20] J. C. Slonczewski, J. Magn. Magn. Mater. **159**, L1 (1996).
[21] L. Berger, Phys. Rev. B **54**, 9353 (1996).
[22] A. Thiaville, Y. Nakatani, J. Miltat, and Y. Suzuki, Europhys. Lett. **69**, 990 (2005).
[23] Z. Li and S. Zhang, Phys. Rev. Lett. **92**, 207203 (2004).
[24] T. A. Moore *et al.*, Phys. Rev. B **80**, 132403 (2009).
[25] A. P. Malozemoff and J. C. Slonczewski, *Magnetic Domain Walls in Bubble Materials* (Academic Press, New York, 1979).
[26] R. Wieser, E. Y. Vedmedenko, and R. Wiesendanger, Phys. Rev. B **81**, 024405 (2010).